

Global Warming and Changes in
Sea Ice in the Greenland Sea: 1979-2007

Maxine von Eye¹

DAMTP, CMS

University of Cambridge

Wilberforce Rd

Cambridge CB3 0WA, UK

M.J.E.v.Eye@damtp.cam.ac.uk, +44 (0)1223 760 398

Alexander von Eye

316 Psychology Building

Michigan State University

East Lansing, MI 48824, USA

voneye@msu.edu

João Rodrigues

DAMTP, CMS

University of Cambridge

Wilberforce Rd

Cambridge CB3 0WA, UK

J.M.Rodrigues@damtp.cam.ac.uk

¹Corresponding Author

Abstract

This paper presents a statistical analysis of sea ice in the Greenland Sea (70-80N and 10W-10E) from January 1979 to December 2007. We define four variables from satellite images: ice extent, ice area, eastward ice extent at 75N, and the shape of the ice edge. We establish relationships between these ice variables and five climate variables: sea surface temperature (SST), air temperature at Jan Mayen Island (JM), sea surface pressure (SSP), North Atlantic Oscillation (NAO) and Arctic Oscillation (AO). The ice extent, ice area and eastward ice extent are highly correlated with SST and JM over the whole time period, while SSP, NAO and AO are only correlated with the ice variables over shorter (one year) periods. When considering the different shapes of the ice edge, an ANOVA model shows that 49% of the variance in extent can be explained by the shape of the ice edge, and similar amounts for the eastward ice extent and ice area. Fourier analysis of the sea ice data shows a 10 year peak which is consistent with previous hypotheses in work done on the Greenland Sea. Finally, we show that the negative trend in the sea ice extent, ice area and eastward extent is statistically significant. This can be interpreted as yet another indicator of the global warming that has been taking place for the last 30 years.

1 Introduction

1.1 Context

Sea ice in the Greenland Sea has been the topic of much research in recent years. The Greenland Sea has long been known as one of only a few open-ocean sites of deep water formation [10, 13], and although the role of sea ice in convection is not fully understood, it is thought that the state of the sea ice can be used to identify convective events [25]. A unique sea ice feature, known as the Odden, is found in the central Greenland Sea in the region of 75°N 0°W . It takes the form of a tongue-shaped protrusion in the North-East direction from the East Greenland ice edge near Jan Mayen Island. The Odden was first documented by sealers who visited the region to hunt harp seal [28]. It has also been thoroughly studied in observational work [27], and variability of the Odden has been discussed using satellite images since 1979 [7, 21, 17].

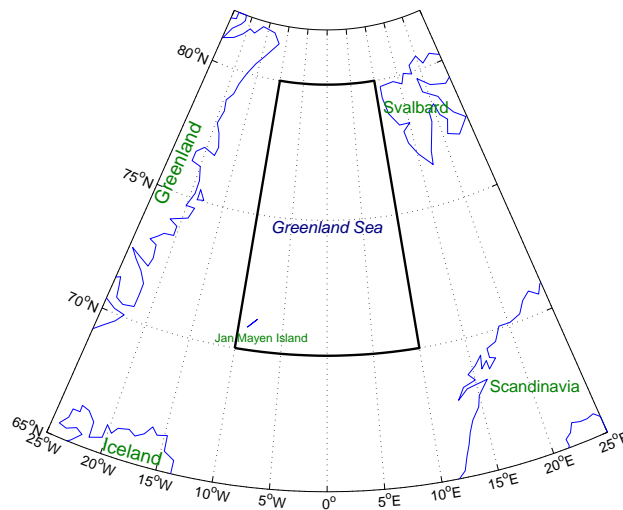


Figure 1: Map of the Greenland Sea Region. Our domain of interest is outlined by a thick black line, from 70 to 80°N and from 10°W to 10°E.

A map of the region is shown in Figure 1. For this study we focus on the domain outlined by a thick black line in Figure 1, from 70 to 80°N and 10°W to 10°E. We choose this domain because (a) it is centered on the Greenland Sea Gyre and the peak of the classically doming isopycnals (surfaces of constant density), (b) it is where the bathymetry is the deepest ($> 2000\text{m}$), and (c) it is the region where the Odden feature is usually observed. The study area includes both locally formed ice in the center of the domain, and some ice that is advected south out of the

Arctic in the East Greenland Current to the west of the domain. Both of these types of ice are important for whether or not convection occurs, and both seem to have been decreasing in recent years. There may be a relationship to global warming, so we include them in this study area. Another implication of this choice of study area is that it borders other areas with different climates or ice regimes, such as areas around Svalbard, Greenland and Iceland. There is no way to avoid a given study area being embedded in a larger region with different climatologies. This will be discussed further in later Sections.

1.2 Previous Work

The Greenland Sea is located at the southern edge of the Arctic sea ice extent, where ice leaving the Arctic through the Fram Strait end up. Sea ice in the Arctic has been shrinking rapidly in recent years [6, 18]. Therefore, we are interested in how sea ice in the Greenland Sea has varied over the past 30 years. There are three main papers which have attempted to analyse historical sea ice data from the Greenland Sea [17, 21, 7].

The authors of [17] analysed sea ice in the Greenland Sea from 1978 to 1995 using a weekly time series in a domain from 70 to 79°N and from 20°W to 6°E. To calculate the amount of ice in the Odden, the authors start by calculating the average ice area in October of each year (what they call the ‘pre-Odden’ ice concentration). This initial concentration is then subtracted from each of the weekly ice areas for the following year. They first look at intra-annual variability by taking the difference between each two consecutive data points and defining Odden growth, Odden decay, stagnant Odden and stagnant no-Odden events. These four cases are then compared with temperature, wind speed and wind direction to determine ‘favourable conditions’ for each case (i.e. the average conditions when these events are happening), and correlation coefficients are calculated for some relationships. Next, the authors look at inter-annual variability; they calculate a number of annual sea ice and climate related variables. They find a lack of correlation between these variables and conclude that “the conditions ... for Odden growth are necessary but not sufficient”. That is, the average conditions they found are not statistically correlated with the events. The authors did, however, find a correlation between the annual maximum ice area and North Atlantic Oscillation and Southern Oscillation Index, but this was not statistically significant. Finally they look at their data in years when deep convection is known to have occurred and conclude that oceanographic data are needed to

make a connection between the Odden and convection more clear.

In [21], the author focuses on the area where the Odden formed in 1993-5, and tries to avoid the ice carried southward by the East Greenland Current. This study considers satellite images from October 1978 to June 1995. The author looks at the ice area for each year and compares it with the weekly average and maximum ice cover. He calculates an integrated ice cover anomaly and suggests a correspondence with the monthly air temperature anomaly in Jan Mayen Island. No statistical analysis is performed and no other climate variables are considered.

The third paper [7] considers a similar study area to the second (not defined explicitly) from 1979 to 1998. The authors quantify the Odden in terms of the daily ice extents in the Odden study area and the whole Greenland Sea, average and standard deviation of the ice concentration, maximum and average ice area and extent, and the sea ice persistence for each year. The ice area is correlated with or simply compared to ice transport through Fram Strait, the temperature at Jan Mayen island, surface temperatures derived from satellite images, and ECMWF winds.

Our results are compared with the results of these previous studies throughout this paper.

1.3 Outline of the Paper

In this paper we use grids of daily sea ice concentration from the National Snow and Ice Data Center (NSIDC) [5, 2]. These data give a daily picture of the state of the sea ice in the Greenland Sea between January 1979 and December 2007, almost 30 years. From these ice charts, we extract several monthly time series: ice extent (percentage of grid cells with ice concentration greater than 15%), ice area (percentage of total area covered by ice), maximum eastward sea ice extent at 75°N, and the shape of the ice edge (monthly maximum longitude where the sea ice crosses 75°N). The time series and the methods used to extract them are discussed in Section 2.

The main focus of this paper is the statistical analysis of these four variables. The goals are (1) to establish whether there are any statistical relationships between the sea ice and other variables and (2) to determine if there are any trends in the state of the sea ice in the Greenland Sea over the past 30 years. To put the state of the sea ice in the Greenland Sea into a larger context, we relate the sea ice time series to a number of climatological time series, the most important being sea surface temperature, air temperature at Jan Mayen Island, sea surface pressure, the North Atlantic Oscillation and the Arctic Oscillation. The results are discussed in

Section 3. The results of this paper are summarised in Section 4.

2 Creating the Time Series

To create our sea ice time series, we use data from NASA satellites carrying passive microwave imaging sensors. The final data sets are distributed by the NSIDC [5, 2]. From 1979 to 1987, we use Scanning Multichannel Microwave Radiometer (SMMR) images; from 1988 to 2002, we use images from the Special Sensor Microwave Imager (SSM/I); finally, from 2003-2007, we use Advanced Microwave Scanning Radiometer (AMSR-E) images. The brightness of each image pixel is converted to a sea ice concentration using the Bootstrap algorithm [3, 4] for SMMR and SSM/I data, and the Enhanced NASA Team algorithm [12] for AMSR-E data. The SMMR data is projected onto a 25 km by 25 km polar stereographic grid, while the SSM/I and AMSR-E data are on a 12.5 km by 12.5 km grid. The error in the data generated using the bootstrap algorithm is 5% in the central arctic and 10% in seasonal ice regions such as the Greenland Sea [3]. It is generally accepted that later data are more accurate [15] although exact error estimates are not given by Markus and Cavalieri [12].

Combining different datasets to obtain a 30 year time series is in accordance with current research practice [15, 7, 21, 17]. Whenever more than one data set is available in for a whole year, we use the images from the more modern instrument. The two algorithms reflect the properties of the data it is used on, and Rodrigues [15] found the difference between SSM/I and AMSR-E data to be small; the difference in sea ice extent and area for the two data sets in 2003 is less than 1% (thus, smaller than the error in generating the data).

From these ice concentration charts we extract four time series:

1. ice extent,
2. ice area,
3. maximum eastward ice extent at 75°N,
4. shape of the ice edge.

The percentage **ice extent** e_{ice} is the percentage of grid cells containing more than 15% sea ice. Because the grid cells all have equal areas, it is calculated by counting the number of grid cells where the sea ice concentration c_k is greater than .15 and dividing by the total number of

all grid cells N , that is

$$e_{ice} = 100 * \sum_{k=1, c_k > .15}^N \frac{1}{N}.$$

It has become convention to define an ice concentration of 15% as the boundary between ice free and ice cover [26, 7, 15]. This is because the accuracy of the sea ice concentrations is $\pm 15\%$ in regions of first-year ice [14], and threshold values of 12% [14] and 14% [8] were used in early observations and analysis. Since we are constructing a monthly time series from these daily images, we take the minimum, mean and maximum value for each month. The results are plotted in Figure 2. The correlations between the minimum, mean and maximum are very high (min and mean $r = .946$, min and max $r = .854$, mean and max $r = .963$) so in this analysis we choose ice extent to refer to the maximum ice extent. Because the correlation between maximum and mean sea ice extent was so high, a recalculation of results led to nearly identical results.

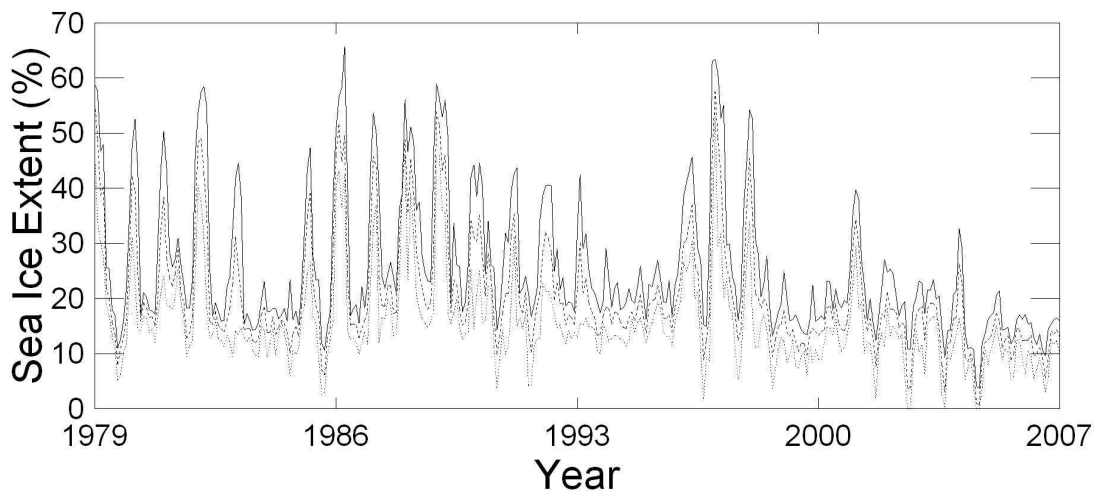


Figure 2: The minimum (dotted), average (dashed) and maximum (solid) sea ice extent in the Greenland Sea from 1979-2007.

The percentage **ice area** measures the percentage of the area covered by ice. It is calculated in a similar way to the ice extent, but the area is weighted by the ice concentration in each grid cell, hence

$$a_{ice} = 100 * \sum_{k=1}^N \frac{c_k}{N}.$$

The minimum, average and maximum are shown in Figure 3. Again, correlations between minimum, mean and maximum are high (min and mean $r = .959$, min and max $r = .869$, mean and max $r = .962$), so we use the maximum ice area in the rest of this paper. The ice extent and ice area were also used in earlier studies of the Greenland Sea [7], and the Arctic region

[15].

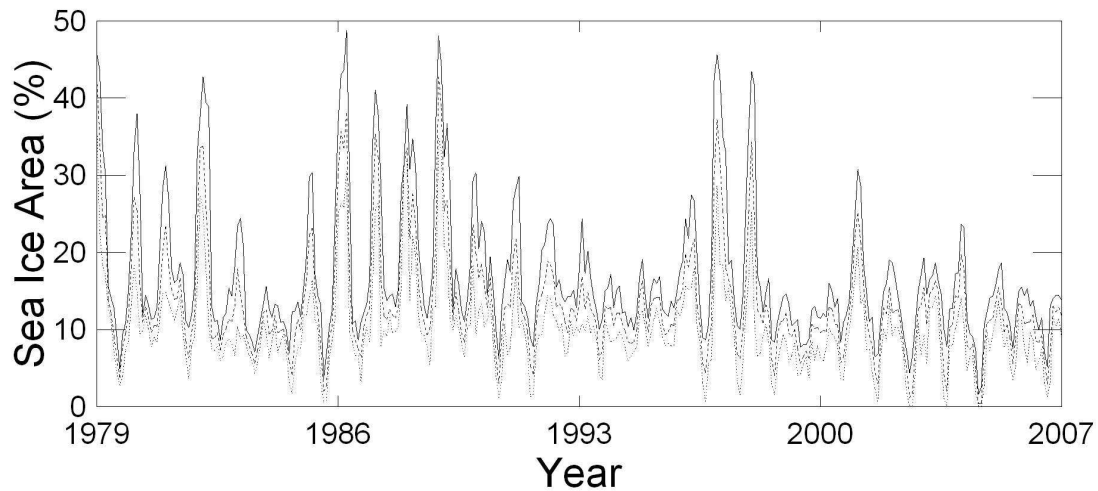


Figure 3: The minimum (dotted), average (dashed) and maximum (solid) sea ice area in the Greenland Sea from 1979-2007.

Sea ice in the Greenland Sea consists mostly of newly formed pancake and frazil ice [27], not continuous ice sheets. This means that the sea ice extent and area in satellite images might be quite different. If the ice distribution is spread out in such a way that most of the grid cells have just over 15% sea ice, then the ice extent would be very large but the ice area would be relatively small. Therefore, we start by considering both variables independently.

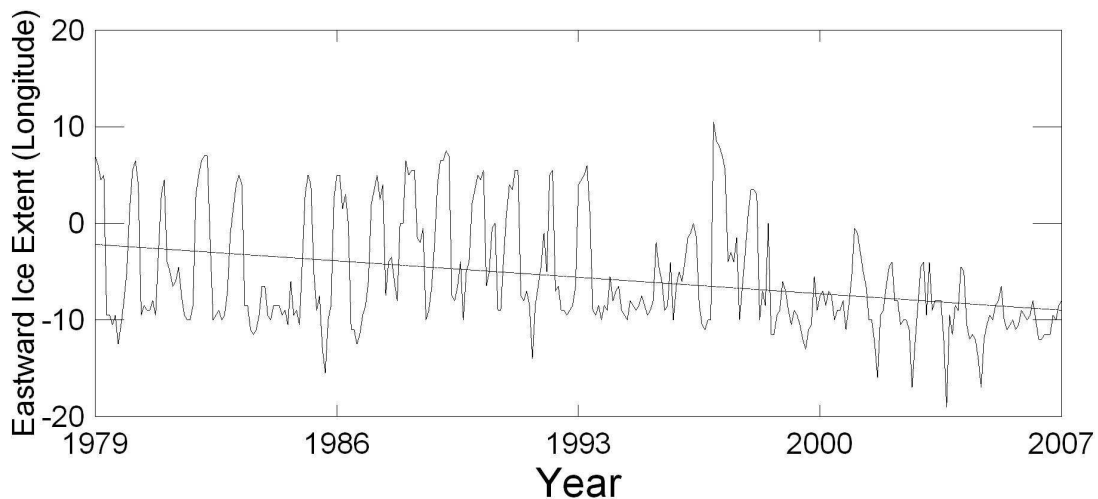


Figure 4: The maximum eastward sea ice extent along 75°N in the Greenland Sea from 1979-2007. The straight line is the trend line over the whole time series.

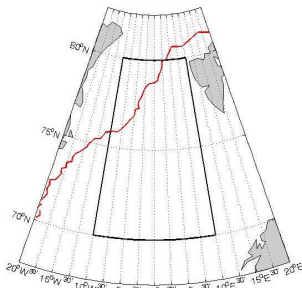
The **maximum eastward extent** of the ice edge at 75°N is the maximum longitude over the whole month where the sea ice crosses 75°N and is shown in Figure 4. For example, in Figures 5a-5e this variable has values -14 , -6 , 4 , 3 , and 4E . Comparing Figures 2, 3 and 4, we

start to see a relationship between these variables. For example, in 1994-1995, the ice extent, ice area and eastward ice extent all have relatively low values, whereas in 1996-1997 all variables have relatively high values. We examine this relationship more rigorously in the next section.

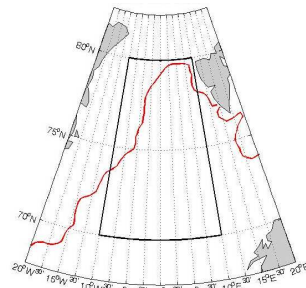
Finally, the **shape of the ice edge** is a categorical variable that can take one of five values

0. no ice in the domain along 75°N ,
1. straight ice edge in domain,
2. bulge from the edge,
3. island detached from the edge,
4. Odden ice tongue.

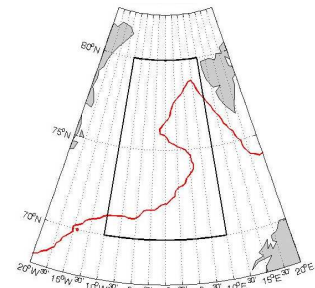
These shape classifications are not intended to be a ranking; they are used as a taxonomy because no natural ranking exists. We define the shape number in such a way that the occurrence of a higher value is of more interest. For example, we are more interested in the occurrence of an Odden ice tongue than a small bulge from the ice edge. Therefore, in each month we take the highest shape classification to have occurred to represent that month.



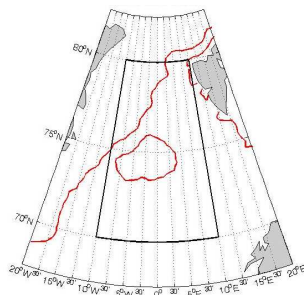
(a) Shape 0, no ice in the domain along 75°N .



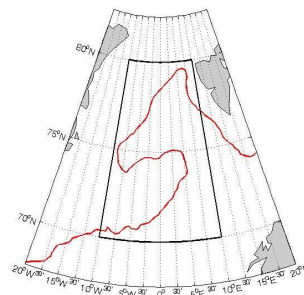
(b) Shape 1, straight ice edge in domain.



(c) Shape 2, bulge from the ice edge.



(d) Shape 3, island detached from the ice edge.



(e) Shape 4, Odden ice tongue.

Figure 5: Examples of the shapes of the ice edge in our domain ($70\text{-}80^{\circ}\text{N}$ and $10^{\circ}\text{W}\text{-}10^{\circ}\text{E}$) of the Greenland Sea.

Examples of these five situations are shown in Figure 5, and the time series is shown in Figure 6. Figure 5b shows an almost straight line through the domain to illustrate the straight ice edge. Figures 5c and 5e show a similar line along where the straight ice edge would be, to demonstrate the protrusion from this edge. The difference between shapes 2 and 4 is that for shape 4 the ice edge doubles back on itself with respect to the straight line, i.e. a line perpendicular to the straight line would cross a bay of ice free water and meet the ice edge a second time. Shape 2 on the other hand is simply a raised area away from the straight ice edge. This raised area, or bulge, can have a range of sizes. It can be a small bump when an Odden is first forming or slowly decaying, or it can be a large bump if the bay of ice free water adjacent to the Odden freezes over. The occurrence of the later type of bulge is discussed in [27]. Although the relationship between the shape variable and the other three ice variables is not yet obvious, as an example we see that all variables have relatively low values in 1994-1995 and higher ones in 1996-1997.

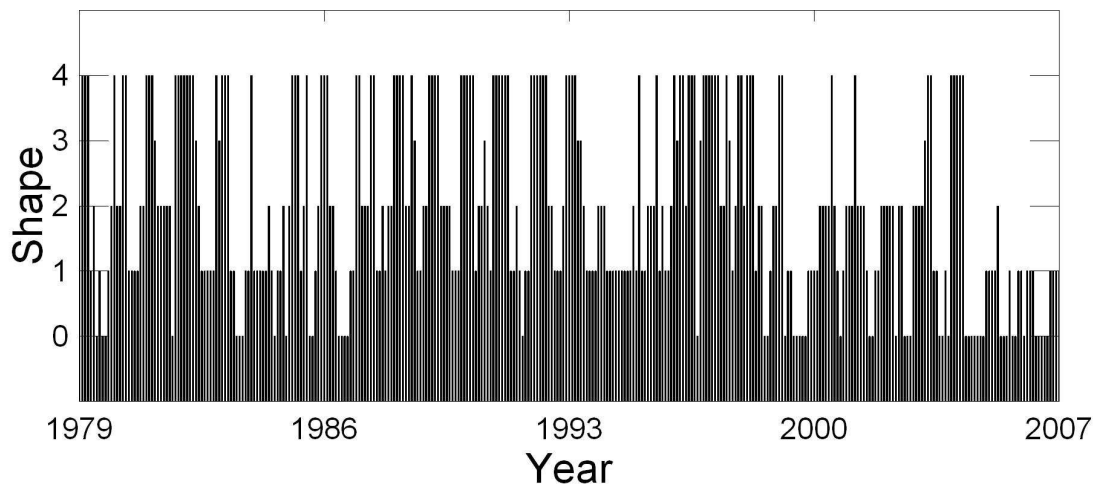


Figure 6: The shape of the ice edge in the Greenland Sea from 1979-2007.

3 Results

In Section 3.1, we correlate the variables defined in Section 2 with one another and look at how the variables differ for the different shapes. In Section 3.2, we correlate the ice variables with other climate variables. A summary of the correlations is shown in Table 1. In Section 3.3, we investigate how these correlations change with time, the periodicity and trends in our data.

3.1 Sea Ice in the Greenland Sea

The first three variables are continuous and can therefore be correlated with one another directly. Figure 7 shows the ice extent, ice area and eastward ice extent plotted against each other. Figure 7 also shows univariate distributions of the variables in each column in the main diagonal of the scatter plot matrix. The correlation between ice extent and ice area is the highest ($r = 0.952$). The linear relationship between these two variables is therefore very strong and it is redundant to talk about both as independent variables. This is visible again, for example, in the plots of the eastward ice extent against the maximum extent and maximum area in Figure 7; the plots look nearly identical and both correlations are high (eastward and ice extent $r = 0.909$, eastward and ice area $r = 0.855$). We restrict ourselves for the rest of this paper to discussing predominantly the sea ice extent. A summary of all the correlations is shown in Table 1.

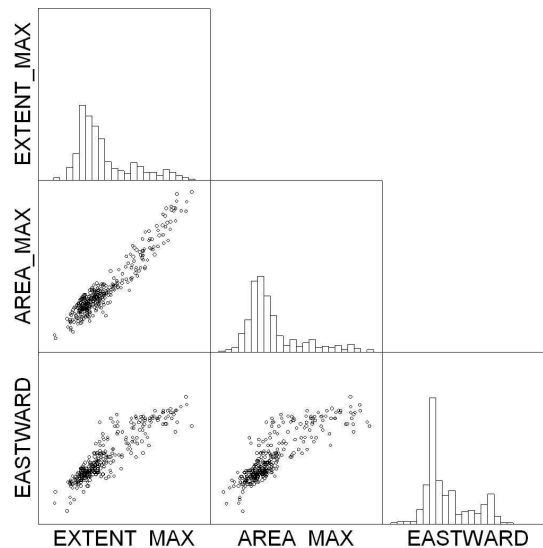
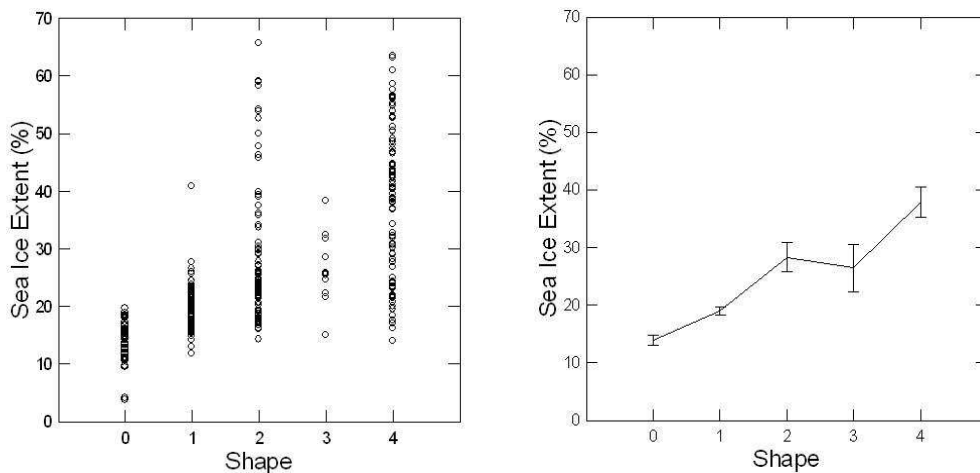


Figure 7: Scatter plots of the ice extent, ice area and eastward ice extent against one another. The histograms along the main diagonal of the scatter plot matrix show univariate distributions of the column variables.

Since the shape of the ice edge is categorical, it does not entirely make sense to correlate it with the other three variables, but the distributions of the other variables by shape are interesting to look at. Figure 8a shows the shape of the ice edge plotted against the ice extent. Here, we see quite a strong relationship. Naturally, for shape 0 (no ice in domain) and shape 1 (straight ice edge), the ice extent is quite small. In contrast, large category numbers indicate a larger ice extent. In fact, the results of an ANOVA model tells us that 49% of the variance in the sea ice extent can be explained by the shape of the ice edge ($F = 80.76, df_1 = 4, df_2 = 343, p <$

0.01, $R^2 = .485$). The variances of the ice extent for the different shapes are heterogeneous, so we use the Games-Howell test to compare the distributions of ice extent by shape. Given two shapes, the mean difference in the sea ice extent for each shape are statistically significant in almost all cases at the 5% level. The exception is the ice extent distributions for shapes 2 and 3. Figure 8b shows the mean ice extent for each shape, and the bars represent the standard errors ($p = .95$). Note that the lines connecting the means do not actually represent values of the eastward ice extent as a function of shape, since shape can only take integer values; instead they represent a difference in the means, with a steeper line representing a larger difference between two consecutive means. In Figure 8b, we can see that the error bars for shapes 2 and 3 overlap, confirming the fact that the difference between them is not statistically significant. ANOVA results are similar for the eastward ice extent ($F = 94.489, df_1 = 4, df_2 = 343, p < 0.01, R^2 = .524$) and ice area ($F = 52.273, df_1 = 4, df_2 = 343, p < 0.01, R^2 = .379$).



(a) Scatter plots of the ice extent plotted against the shape of the ice edge. (b) Mean ice extent and 95% standard error bars.

Figure 8: Ice extent by shape.

	ice extent	ice area	eastward
ice extent	1.0		
ice area	.952	1.0	
eastward	.909	.855	1.0
SST	-.562	-.633	-.583
JM	-.655	-.713	-.654
SSP	.135	.130	.198
NAO	.080	.049	.120
AO	.062	.024	.071

Table 1: Summary of correlations between ice variables and climatological variables.

3.2 Correlation with Climatological Data Sets

In order to put the sea ice data from the Greenland sea into a larger context, we correlate our ice data with climatology data from various other sources:

1. HadISST sea surface temperatures (SST),
2. Jan Mayen Island air temperatures (JM),
3. GMSLP sea surface pressures (SSP),
4. North Atlantic Oscillation (NAO),
5. Arctic Oscillation (AO).

Some of the correlations are (not surprisingly) relatively large for variables that have a clear seasonal cycle, and small for variables without a clear seasonal cycle. In the cases where a seasonal cycle is prominent, we gain additional insight by also considering correlations with monthly anomalies. For a given month the anomaly of a variable is defined as the value of that variable minus the average of that variable in that month over all the years (1979-2007). For example, the SST anomaly in January 1980 is the SST value in January 1980 minus the January average from 1979 to 2007. This is a common technique used to detrend climate data.

3.2.1 Sea Surface Temperature

The Sea Surface Temperature, **SST**, is a $1^\circ \times 1^\circ$ globally gridded, monthly data set [23]. In order to use these data with our Greenland Sea ice data, we average the temperature over the whole domain; if ice cover was present, we set the temperature to the freezing point -1.9°C . The temperatures are shown in Figure 9 (solid line). The correlation between SST and ice extent, ice area and eastward ice extent are -0.562 , -0.633 , and -0.583 respectively; as the sea surface temperature increases, the values of these variables all decrease, which can be seen in the scatter plots in Figure 10. A large correlation does not mean that one variable implies the other, simply that they covary. In this case, heat loss to the atmosphere, or cooling, causes both the low SST and the freezing to occur. The authors of [7] found slightly higher correlations between ice area and surface temperature derived from satellite images ($r = -.89$); this may be due to the fact that their surface temperature depends on the extent of the ice cover. If the SST time series is shifted either direction in time with respect to the ice time series (cross-correlation, not shown),

then the correlation drops. This again indicates that the ice extent, ice area and eastward ice extent covary with the sea surface temperature.

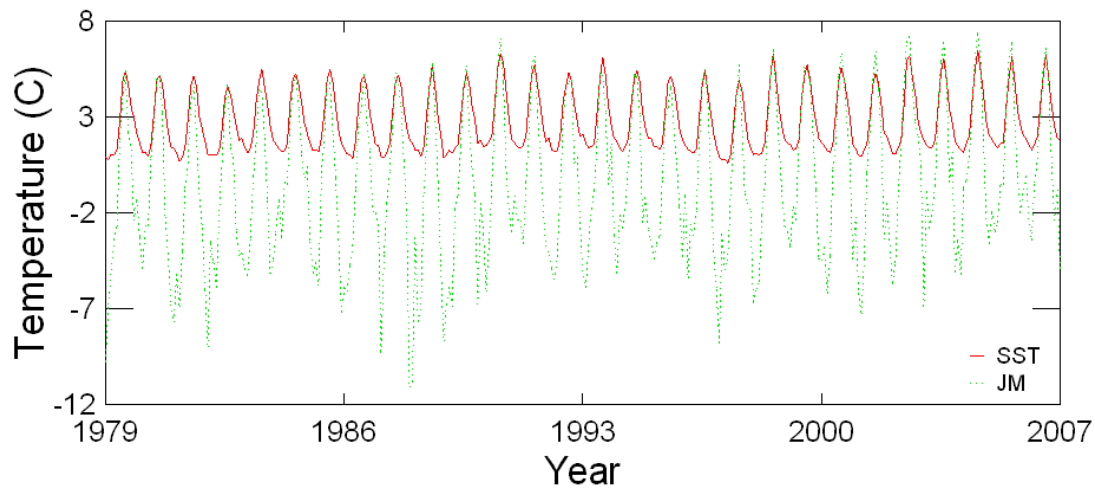


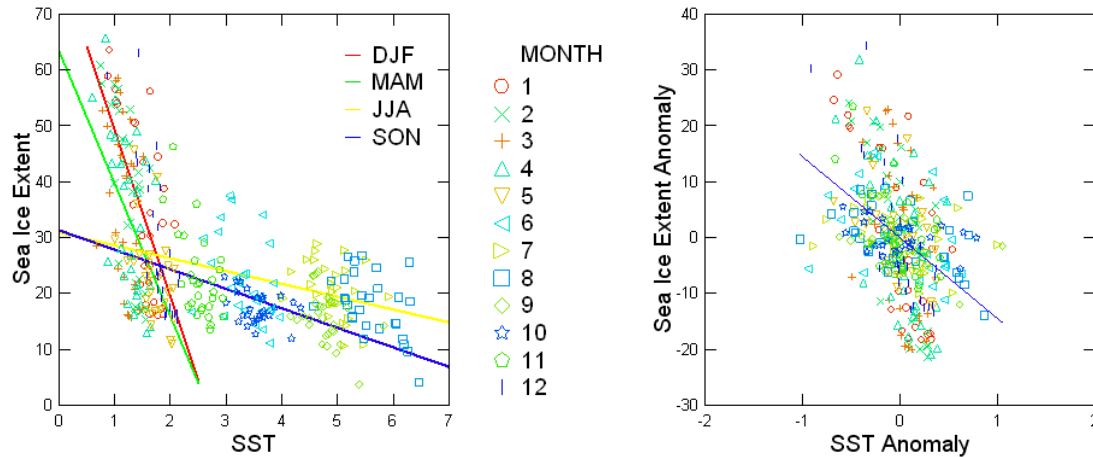
Figure 9: The SST (solid) and JM (dashed) temperature time series. SST is plotted from 1979-2007, while JM is from 1979-2007.

In Figure 10a, we can see that a linear trend line that covers the entire range of SST does not fit the data well. At low temperatures, the sea ice extent is very high but drops rapidly as the temperature increases to approximately 2°C . Above that temperature, sea ice extent decrease slightly. This change in the trend is demonstrated by the solid best fit line in Figure 10a which changes from very steep (red) to very shallow (yellow) near 2°C for the ice extent and SST. In fact, this change in the trend is related to the time dependence in the Figure. The different shaped points in Figure 10a represent the data from different months. The steep slopes are data from December to February (red, slope = -29.8% per $^{\circ}\text{C}$) and March to May (green, slope = -23.7% per $^{\circ}\text{C}$), while the shallower slopes are data from June to August (yellow, slope = -2.3% per $^{\circ}\text{C}$) and September to November (blue, slope = -3.5% per $^{\circ}\text{C}$). In the winter (December to May), the water is generally close to the freezing point and the amount of ice varies a lot to give a steep slope. In the summer (June to November), on the other hand, there is not much ice and a larger range of water temperatures, which results in a shallower slope. The four slopes in Figure 10a indicate that there are in fact only two seasons observed in the Greenland Sea.

SST Anomalies

Considering the monthly anomalies of both the ice data and SST eliminates the variation due to the seasons. Figure 10b shows the SST anomalies plotted against extent anomalies, with different shapes still representing different months. The correlation between SST anomalies and

ice extent, ice area and eastward ice extent anomalies are $-.321$, $-.452$ and $-.458$ respectively; for example if SST is larger than average in a given month then the sea ice extent is smaller than average, as expected. These correlations are smaller than the correlations in the raw data because they do not include the seasonal cycle.



(a) SST plotted against sea ice extent with trend lines for winter (DJF), spring (MAM), summer (JJA) and autumn (SON).

(b) SST anomalies plotted against sea ice extent anomalies with trend line for all 12 months.

Figure 10: Scatter plots of SST against sea ice extent. Different shaped data points representing different months to show the time dependence of the relationship.

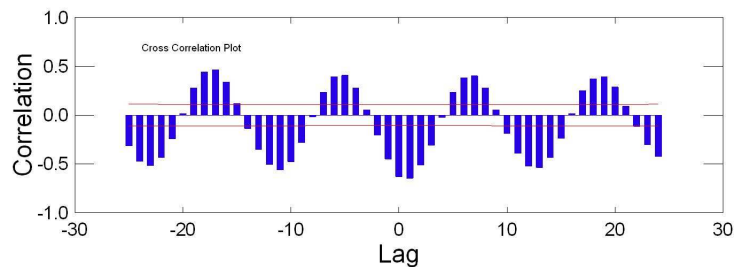
3.2.2 Air Temperature

Jan Mayen Island is located in the south west corner of our domain, at approximately 71°N 8°W ; it is the only weather station inside the domain. An in situ air temperature record, **JM**, had been kept monthly since 1921 until 2001 [22] and more recently by the Norwegian Met Office [9], which is plotted (dashed line) for our time period in Figure 9. The air temperatures on Jan Mayen Island have a much larger range than the SSTs (because the SST is bounded below by the freezing point), but the amplitudes of the peaks in the two time series match quite well; indeed, the correlation between these two time series is .886.

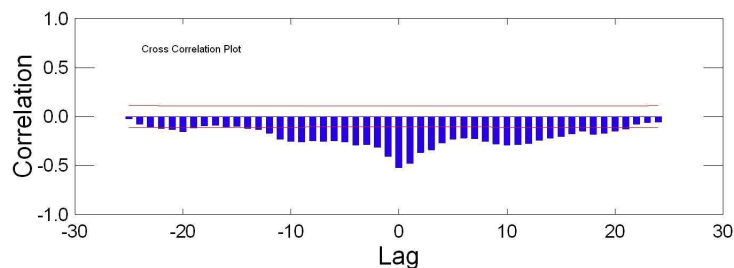
Scatter plots (not shown) of JM against the ice variables show a similar trend to those for SST. The change in slope is not as sharp as for SST, so the correlations between JM and ice extent, ice area and eastward ice extent are stronger than the correlations with SST ($r = -0.632$, -0.707 , -0.641 respectively). The authors of [17] found correlations of $-.29$ and $-.68$ over shorter time periods of one year and 6 weeks, but their analysis did not find a correlation between Odden growth and meteorological data for their entire period (1979-1995).

The authors of [7] on the other hand, also found a strong correlation between monthly average ice area and air temperature at Jan Mayen Island ($r = -.74$) between 1979 and 1998.

Although the correlations we find are high, if JM is cross-correlated with ice extent and eastward ice extent, the peak in correlations is not at zero lag (as it is for SST). Figure 11 displays the cross-correlation between the ice extent and JM and shows that the peak in the cross-correlation is when ice extent is lagging behind JM by one month. The results are the same for eastward ice extent (not shown). A natural interpretation of this is that it takes up to one month for changes in the air temperature to manifest themselves into changes in the sea ice extent, but the difference in correlations between lag 0 and lag 1 is not statistically significant ($t = .598$, $df = 347$, $p = .275$) and so it could be due to chance.



(a) The peak is at ice extent lagging JM by one month.



(b) The peak is at zero lag between ice extent anomaly and JM anomaly.

Figure 11: Cross-Correlation of JM with eastward ice extent and JM anomaly with eastward anomaly. Lag is shown in months. Correlations that extent above (or below) the horizontal lines are statistically significant.

What is interesting is that the sea ice area does not behave the same way. The peak in the cross-correlation of JM with sea ice area (not shown) has the largest peak at zero lag, which means that the ice area responds more quickly to changes in the air temperature than ice extent does. The fact that ice area seems to responds more quickly to changes in temperature than sea ice extent and eastward ice extent is due to the definition of these variables. As the temperature increases and ice melts, the ice area (variable) will decrease immediately because the total area

covered by ice is decreasing; the sea ice extent on the other hand will not decrease until the ice concentration reaches the 15% threshold and the number of grid cells with less than 15% ice decreases. The cross correlation also has positive peaks at -5 and 7 months, which are indicative of the annual cycle; if JM is shifted 6 months in either direction from the main peak with respect to the eastward ice extent, then a peak in temperature (summer) would correspond to a peak in ice extent (winter) giving a strong positive correlation.

Other air temperature records also exist in the Nordklim data set [22]. After JM, which is in our domain of interest, Akureyri and Stykkisholmur in Iceland, and Svalbard Airport are the next nearest weather stations. As mentioned in the introduction (Section 1.1), these stations lie outside our study area in what might be very different climates and ice regimes. It is therefore interesting to determine the relationship, if any, between ice in the Greenland Sea and the climate in surrounding areas. The correlations between our ice variables and air temperature are medium at Akureyri, medium to high at Stykkisholmur and highest at Svalbard; a summary is shown in Table 2.

	Jan Mayen	Svalbard	Stykkisholmur	Akureyri
extent	-.632	-.590	-.487	-.461
area	-.707	-.674	-.544	-.528
eastward	-.641	-.599	-.521	-.492

Table 2: Correlations between air temperature at different weather stations and three sea ice variables.

Air Temperature Anomalies

Since the above correlations with JM depend on the seasons (i.e. different slopes in summer and winter), we again calculate the monthly anomalies in JM. The correlations between JM anomalies and sea ice extent, sea ice area and eastward ice extent anomalies are $-.523$, $-.517$, and $-.350$ respectively.

Some of the correlation at the other weather stations is also due to the seasonal cycle of the data, so correlations of monthly anomalies are also shown in Table 3. The correlations are medium at Svalbard, low at Stykkisholmur and nearly zero at Akureyri. Therefore, in addition to JM, the air temperature at Svalbard is a good indicator of the state of the sea ice in the Greenland Sea. Since Svalbard is just outside the domain to the north-east, these high correlation imply that some of what is happening in the Greenland Sea is due to weather coming from the north out of the Arctic.

	Jan Mayen	Svalbard	Stykkisholmur	Akureyri
extent	-.341	-.457	.107	.036
area	-.453	-.465	.126	.027
eastward	-.478	-.379	.115	.031

Table 3: Correlations between air temperature anomalies at different weather stations and three sea ice variable anomalies.

3.2.3 Sea Surface Pressure and Wind

The Sea Surface Pressure, **SSP**, is a $5^\circ \times 5^\circ$ gridded, monthly data set [1]. We take the grid cells centered at $75^\circ\text{N } 0^\circ\text{W}$ to get a monthly pressure time series, shown in Figure 12a. This time series looks a bit different from the others because the seasonal trend is not as strong. The correlation with our ice variables is very low (ice extent $r = -.121$, ice area $r = -.145$, eastward extent $r = -.146$). The small eccentricity of the 95% confidence ellipse in Figure 12b shows that there is a weak relationship between SSP and sea ice extent, and the orientation shows the correlation is negative. The authors of [17] also found atmospheric pressure not to be significantly related to any ice growth or decay events.

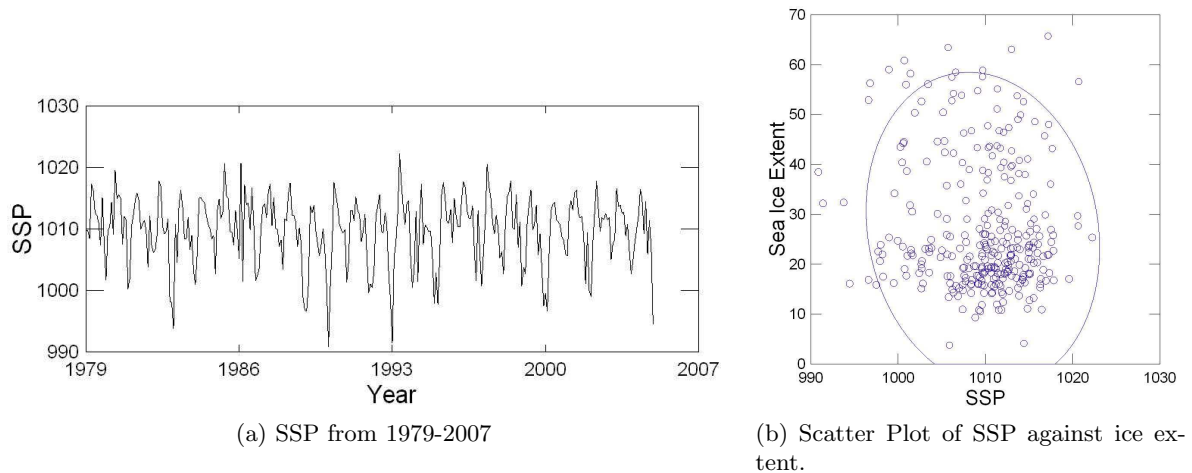


Figure 12: Time series and scatter plots of SSP.

In addition to the SSP at one location, the HadSLP2 data set [1] can be used to calculate the difference in pressure between two locations, which is a proxy for the strength of the wind. We calculate the pressure difference between 10°W and 10°E along 70° , 75° and 80°N as a proxy for the northerly winds. The correlations between these and the ice variables are summarised in Table 4. It is interesting to note that the highest correlations are with the pressure difference at 80°N ; this indicates that the wind which pushes ice through Fram Strait is an important factor in determining the state of the sea ice in the Greenland Sea.

We also calculate pressure difference between 70 and 80°N along 10°W, 0° and 10°E as a proxy for the westerly winds. The correlations (Table 4) are highest (although still quite low) along 10°W, which implies that the wind blowing ice away from the east Greenland ice edge is the most important. In this case, though, the correlations are negative so a larger pressure difference indicates less ice. In other words, strong winds or storms are blowing the newly formed ice away.

	70°	75°	80°		10°W	0°	10°E
70°	1			10°W	1		
75°	.667	1		0°	.938	1	
80°	.491	.828	1	10°E	.860	.921	1
ice extent	.083	.234	.324	ice extent	-.128	-.071	-.139
ice area	.138	.320	.400	ice area	-.196	-.139	-.060
eastward	.122	.261	.355	eastward	-.179	-.120	-.058

(a) Correlations with pressure difference between 10°W and 10°E along 70, 75 and 80°N.

(b) Correlations with pressure difference between 70 and 80°N along 10°W, 0° and 10°E

Table 4: Correlations between pressure differences and sea ice area, sea ice extent and eastward sea ice extent.

SSP Anomalies

Even though SSP does not have a strong seasonal cycle, we still consider briefly the SSP anomalies. The SSP anomaly correlations with sea ice extent, sea ice area and eastward sea ice extent anomalies are .112, .170 and .078 respectively. These are just as low as the correlations between the raw data, so offer no additional insight.

3.2.4 North Atlantic and Arctic Oscillation

The North Atlantic Oscillation, **NAO**, is defined as the pressure difference between Iceland and the Azores. Monthly and annual values are available from 1821-2007 [24]. Again, we see very little seasonal trend in this time series, and the correlation with our ice variables is very low (ice extent $r = .080$, ice area $r = .049$, eastward extent $r = .120$). This is an interesting result because the authors of [17] and [7] found correlations of .42 and .4 respectively for the periods of 1979-1995 and 1979-1998, which we are unable to reproduce with our data.

Finally, the Arctic Oscillation (**AO**) refers to non-seasonal air pressure patterns in the mid- to high- northern latitudes. A negative phase exhibits high pressures in the polar regions, while a positive phase exhibits low pressures. A monthly data set is available from 1899 to 1997

[19, 20]. It has low correlation with our sea ice variables (ice extent $r = .062$, ice area $r = .024$, eastward extent $r = .071$). The low correlation between our ice variables and SSP, NAO and AO indicates that the state of the sea ice is not related to the local or regional atmospheric circulation over such a long time period.

NAO and AO Anomalies

The correlations between NAO and AO anomalies and the sea ice variables are just as low as the raw data, and therefore add no additional insight to the analysis. The NAO anomaly correlations with sea ice extent, sea ice area and eastward sea ice extent anomalies are $-.071$, $-.119$ and $-.030$ respectively. The AO anomaly correlations with sea ice extent, sea ice area and eastward sea ice extent anomalies are $-.028$, $-.082$ and $-.016$ respectively.

3.3 Inter-Annual Variability and Global Warming

Changes in Correlation

In Sections 3.1 and 3.2, we discussed how the different ice and meteorological data sets are correlated with one another over the whole period from 1979-2007, and a summary was given in Table 1. Now, we consider how these correlations change with time. Figure 13 shows the correlation between the ice extent and SST, JM, SSP, NAO, and AO for each year from 1979 to 2007. The plots for ice area and eastward ice extent look very similar, so they are not shown here. First of all, we see that the behaviour of the correlations with SST and JM are nearly identical. The correlation fluctuates between approximately $-.5$ and $-.9$ as expected, except for in 1984 and 1994-5 when the correlations are much weaker. These years are among those in which the ice variables have very low values in the winter (see Figures 2, 3 and 4); there are no other indicators for why these years are different from the rest.

The correlations with NAO and AO behave in the same way, and in a way opposite to the correlation with SSP; when the correlation with NAO and AO has a peak, then the correlation with SSP has a trough. The behaviour of these variables is very different from JM and SST. For NAO, AO and SSP, the fact that there is no correlation over the whole time period obscures the fact that correlations exist over shorter periods. The correlations fluctuate much more dramatically, between $-.82$ and $+.82$. It seems that over shorter time periods (one year) the correlation between ice extent and SSP, NAO and AO is very strong, while over the whole time period (29 years) the correlation is nearly zero. There are no trends in any of these correlations.

An explanation still needs to be found for these annual changes in correlations.

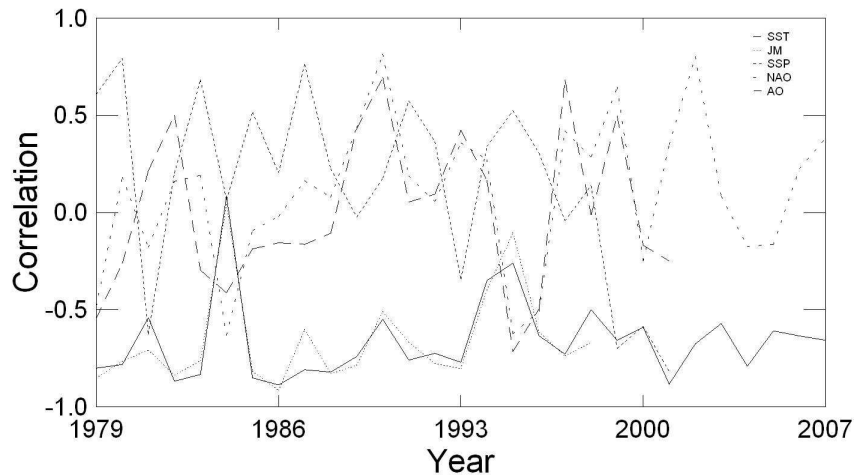


Figure 13: Plot of how the correlation coefficients of the eastward ice extent with SST, JM, SSP, NAO and AO change for each year between 1979 and 2007.

Periodicity

A 10-year periodicity of the ice in the Greenland Sea has previously been suggested [17, 7]. A similar period (11 years) has also been found in other climate variables, such as rainfall, and has been linked to sun spot cycles [16]. Here we examine this in our data. Figure 14 shows the Fast Fourier Transform (FFT) of the eastward ice extent (shown in Figure 4). (Before taking the FFT we subtract off the mean of the whole time series from each value to eliminate the zero frequency component, which often has a high yet uninteresting peak.) The FFT has three dominant peaks at frequencies $.0029$, $.0086$ and $.0833 \text{ months}^{-1}$. The first corresponds to a period of 348 months, or the entire length of our time series. This can be seen in Figure 4 because the first half of the time series has higher values than the second half. The negative trend line for the time series is also plotted in this figure as a straight line. The second peak (circle) corresponds to a period of 116 months, the closest frequency bin to a 10 year period. This agrees with the 10 year periodicity suggested in previous papers. The third and largest peak (triangle) corresponds to a period of 12 months; this is the annual cycle.

Two features in the eastward ice extent may cause the time series to be non-stationary. First, the seasonal cycle; the mean eastward sea ice extent in January is larger than that in July. To eliminate this trend, we again use anomalies so that the mean in each month is zero. Second, the eastward sea ice extent (and the eastward sea ice extent anomalies) decrease with time. (Trends in the data will be discussed in more detail later in this section.) To eliminate

this negative trend, we subtract the best fit line from the eastward sea ice extent anomalies, so that the mean is zero throughout the time series. The resulting detrended eastward sea ice anomalies are shown in Figure 14b. Notice that the first peak at a period of 348 months is still present even though we removed the linear trend from the data, which indicates that a 30 year period may also be present. We see that the peak corresponding to an annual cycle (triangle) has been removed, and the 10 year peak (circle) has grown relative to the rest of the spectrum.

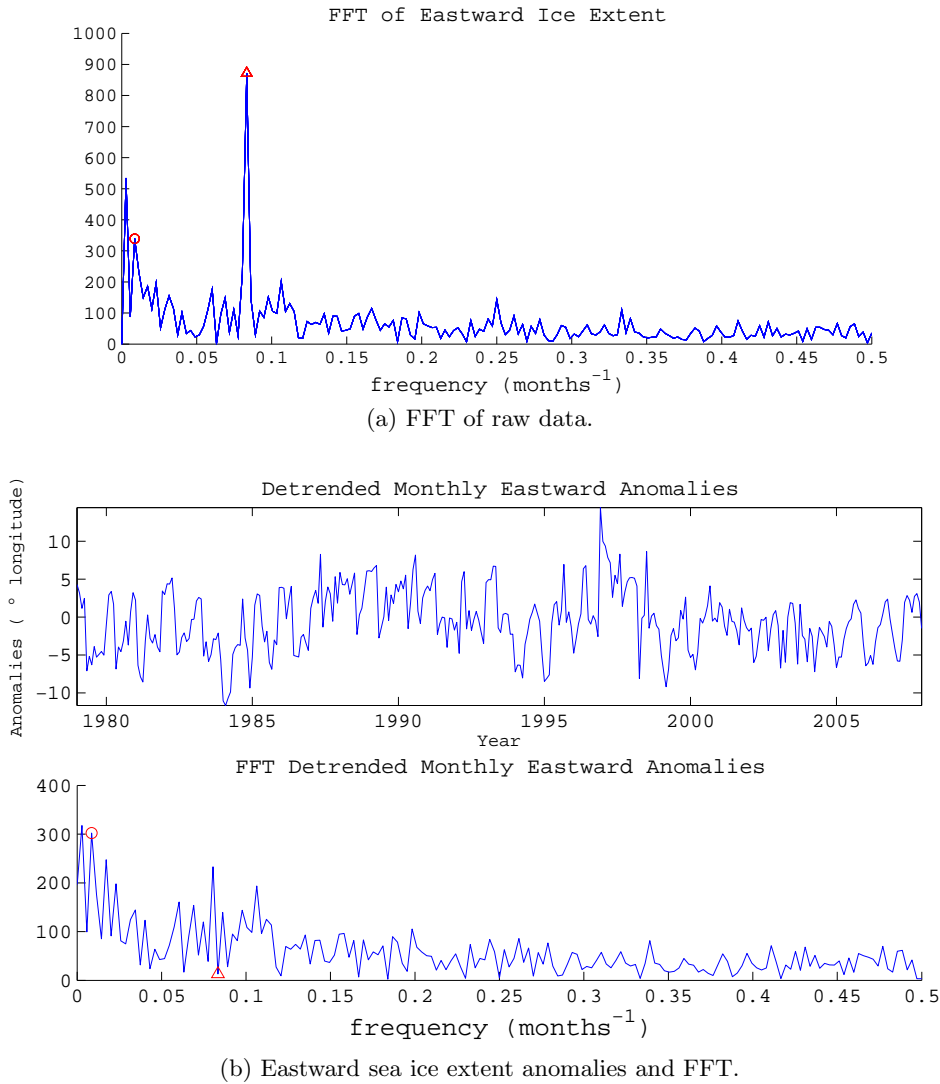


Figure 14: FFT of eastward ice extent. The circle and triangle show the peaks at 10 years and 1 year respectively.

Trends

In addition to the periodicity of the time series, we would like to look at trends over the 29 year period. Figures 15 and 16 show how SST and the ice extent have changed over the time period for each month. First, in the SST plots, we see slight warming trends for all 12 months (slopes

= .010, .011, .008, .015, .008, .014, .020, .036, .014, .014, .004 and .010 degrees per year for Jan - Dec). The trend is strongest in the summer months, but is quite consistent throughout the whole year. Investigating whether there is a change in the SST over the years, we find that the changes in February, April, July and August are statistically significant. (This depends not only on the slope of the line, but also on the standard error or scatter of the data points; therefore the largest slopes are not necessarily the ones that will be statistically significant.) The trends in the other eight months are not statistically significant, which means that they could be due to chance rather than some systematic change such as global warming.

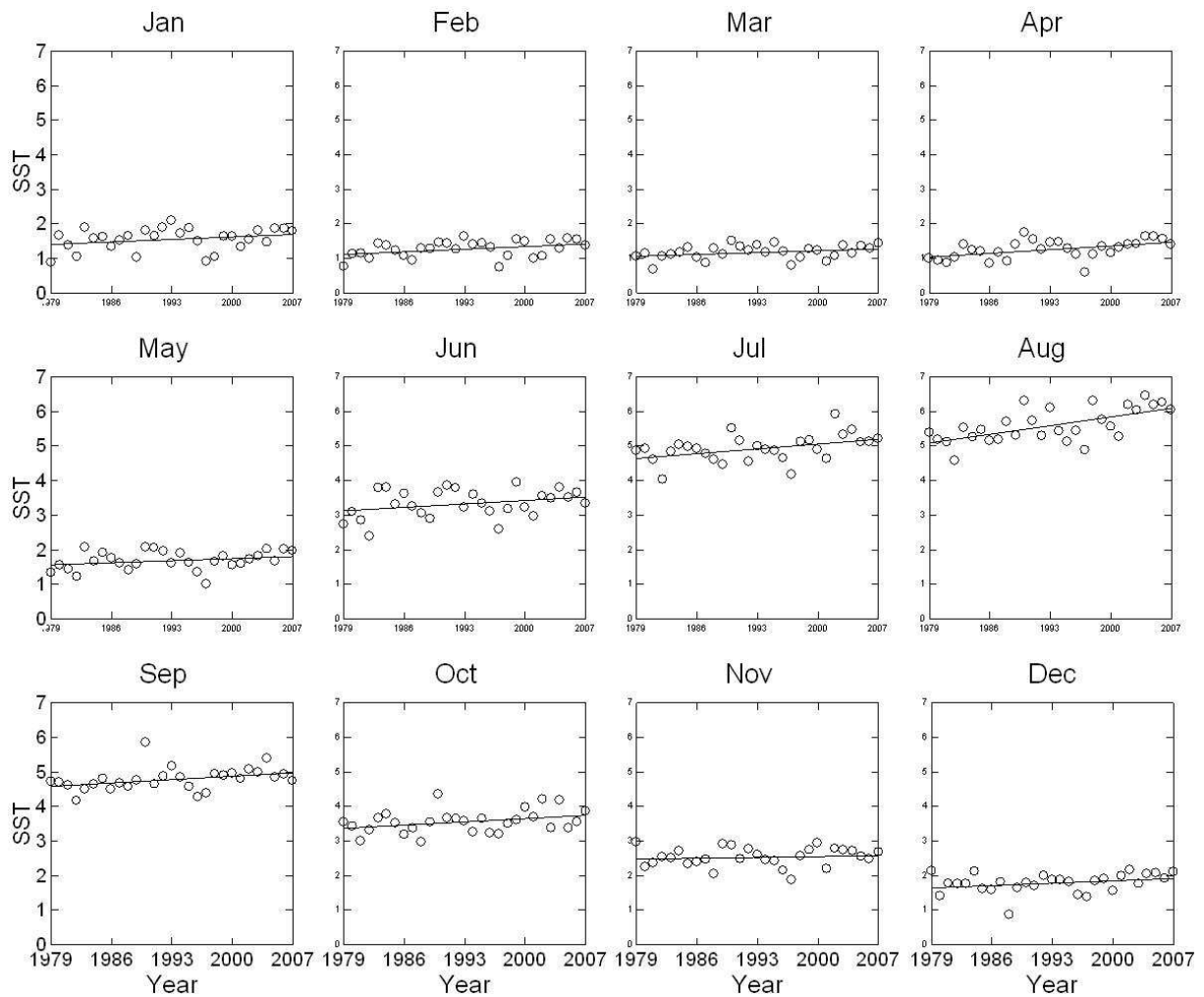


Figure 15: The SST plotted for each month, from 1979 to 2007. A warming tend is seen in SST for each month, but is only statistically significant in February, April, July and August.

There is a positive trend (.017 degrees per year) in the data when all the months from 1979-2007 are taken together. This trend is not statistically significant. An inspection of the residuals shows that they are not symmetric about the regression line. Therefore, we rank transform the

SST data (such that the lowest value has rank 1, the second value has rank 2 and so on to the highest value which has rank 348). A reanalysis of the regression results in a statistically significant positive trend (1.36 rank per month), with a symmetric residual distribution.

The results for JM look very similar, but only the trends in July, August and September are statistically significant. The overall slope in neither the raw data, nor the rank transformed data is statistically significant.

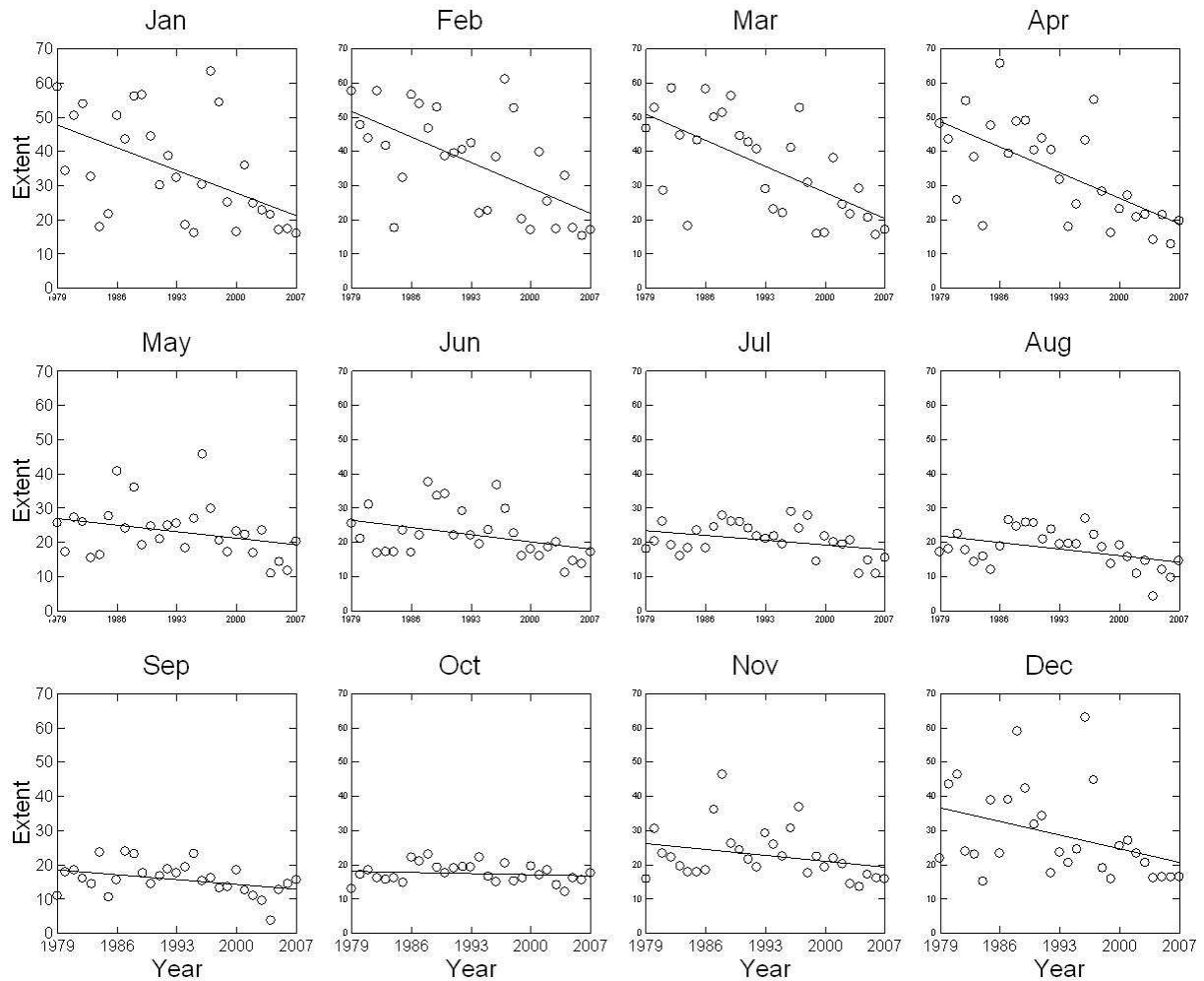


Figure 16: The ice extent plotted for each month, from 1979 to 2007. A decline in the percentage ice cover is seen in all months, but only December to April, August and September are statistically significant.

A much more dramatic result is seen in the trends of the sea ice extent for each month over our time period (Figure 16). Here we see a very strong decline in the sea ice extent in the winter (Dec, Jan, Feb, Mar, Apr slopes are -0.569 , -0.947 , -1.066 , -1.090 , -1.067 % per year), all of which are statistically significant. A smaller decline is found in the summer (May-Nov slopes are -0.274 , -0.302 , -0.199 , -0.274 , -0.201 , -0.047 , -0.246 % per year) where only August and September

are statistically significant. This means that the decline in sea ice extent for a number of months is not due to chance. Overall, the decrease in sea ice extent from 1979 to 2007 of -0.544% per year is statistically significant. Similarly, the decrease in sea ice area and eastward ice extent is statistically significant in only January to April, and January to April, September, November and December respectively. The only month where the trend is not negative is for the sea ice area is October, but this positive trend is not significantly significant. The overall decrease in both these variables is also statistically significant.

Finally, using the shape of the ice edge, we can derive other yearly data sets such as the number of months a given shape category is observed in a year. These time series are shown in Figure 17. Given that only one shape is recorded per month, a negative linear relationship is expected between the number of Oddens and the number of all other shapes combined. What is surprising is that years with a large number of Odden shapes (shape 4) have a small number of straight ice edges (shape 1). Indeed there is a negative correlation between these two variables ($r = -0.765$), while the other shapes are relatively uncorrelated with one another. There is no trend in the number of observations of the different ice edges.

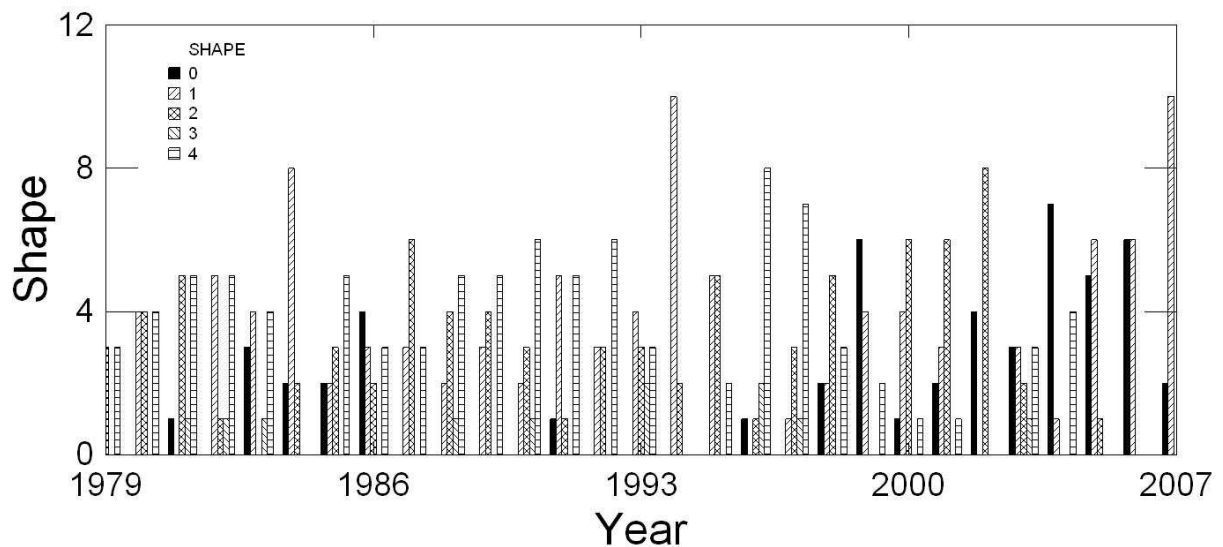


Figure 17: The number of observations of each shape by year from 1979 to 2007.

4 Discussion and Summary

In this paper, we performed a new statistical analysis on sea ice data from the Greenland Sea. The study area chosen in this work is different than those in previous studies of ice in the

Greenland Sea. It is smaller than that used by Shuchman [17] so it includes less of the East Greenland marginal ice zone. Figure 1 in [11] shows that ice west of 10°W along 75°N is between 1-7 years old, and therefore it is too old and too far west to affect the forcing of convection in the central Greenland Sea. Toudal [21] on the other hand, focuses his study on a much smaller domain than ours, where the Odden formed in 1993-5. Due to the large variability in the size and location of the Odden over the past 30 years, we found such a small domain too restrictive.

In our domain, we discussed four variables that describe the state of the sea ice in the Greenland Sea: maximum ice extent, maximum ice area, eastward ice extent along 75°N and the shape of the ice edge. We started by considering how the three ice variables depend on the shape of the ice edge, and found that the differences in the distributions of ice variables for the different shapes are statistically significant. We also found that approximately 50% of the variability in the ice extent, ice area and eastward ice extent can be explained by the shape of the ice edge.

Next, we correlated our three ice variables with several climatological data sets: sea surface temperature (SST), air temperature at Jan Mayen Island (JM), sea surface pressure (SSP), north Atlantic oscillation (NAO), and Arctic Oscillation (AO). A summary of the correlations can be found in Table 1. Over the whole time period from 1979 to 2007 the sea ice extent, sea ice area and eastward ice extent are very highly correlated with the temperature variables, SST and JM, and medium to high correlations with air temperature at Svalbard. The correlation with the other variables on the other hand is low. The SSP data were also used to calculate pressure differences in the domain (as a proxy for wind), and we found medium correlations between the ice variables and the pressure difference between 10°W and 10°E along 80°N and the pressure difference between 70 and 80°N along 10°W .

Although the correlation of the ice time series with SSP, NAO and AO were low over the whole 29 year time span, they were not low when correlations were calculated by year. In fact, the correlations fluctuated between very positive and very negative. For the eastward ice extent, for example, the correlation varied between $-.631$ and $+.814$. There is no obvious trend in the correlations of these variables, and no association with the shape of the ice edge or the appearance of the Odden.

A 10-year periodicity of the ice in the Greenland Sea had been suggested in previous work. By taking a FFT of our sea ice data, we confirm that there is a peak at a frequency of .0086

months⁻¹, which is the closest bin to a 10 year period.

Finally, we looked at trends in the variables from 1979 to 2007. One of the big questions in climate science today is whether global warming is happening or not, and we wanted to see what our results say about this question. A negative trend was found in almost all months, and overall, for the three sea ice variables. This trend is statistically significant for all three variables in January to April, and overall. The trend in temperature on the other hand is positive, but only the trends in July and August are statistically significant for both JM and SST. For SSP, NAO and AO there is no general trend in an month or overall, and none are statistically significant.

We set out two goals in Section 1.3. First we wanted to determine if a statistical relationship exists between the sea ice in the Greenland Sea and other climate variables. The sea ice variables in the Greenland Sea are the most strongly correlated with sea surface temperature and air temperature at Jan Mayen Island. Second, we wanted to find any trends in these variables. We found that there has been a statistically significant decrease in the sea ice extent, sea ice area and eastward sea ice extent at 75°N from 1979 to 2007.

The goal of future work would be to extend the time series back to before the satellite era. Having a historical time series of ocean properties would be necessary to determine any link between the state of the sea ice and convection in the Greenland Sea. The role of sea ice in convection in the Greenland Sea is still an open question. Convection modifies the temperature and salinity properties of the ocean, and time series of these properties need to be correlated with ice time series to see if there is a relationship between the two.

Acknowledgements

Support for MvE came from a grant awarded to Astrid Ogilvie (INSTAAR, University of Colorado) from the National Science Foundation (0629500).

References

- [1] R. J. Allan and T. J. Ansell. A new globally complete monthly historical mean sea level pressure data set (hadslp2): 1850-2004. *Journal of Climate*, (accepted), 2006.
- [2] D. Cavalieri and J. Comiso. *AMSR-E/Aqua daily L3 12.5km Tb, sea ice concentrations and snow depth polar grids*. National Snow and Ice Data Center, Boulder, CO, 2004. Digital Media (updated daily).
- [3] J. Comiso. Characteristics of arctic winter sea ice from satellite multispectral microwave observations. *Journal of Geophysical Research*, 91:975–994, 1986.
- [4] J. Comiso. SSM/I sea ice concentrations using Bootstrap Algorithm. In *NASA ref. Publication 1380*. 1995.

- [5] J. Comiso. *Bootstrap sea ice concentrations from Nimbus-7 SMMR and DMSP SSM/I*. National Snow and Ice Data Center, Boulder, CO, 1999. Digital Media (Updated 2008).
- [6] J. C. Comiso, C. L. Parkinson, R. Gersten, and Larry Stock. Accelerated decline in the Arctic sea ice cover. *Geophysical Research Letters*, 35:L01703, January 2008.
- [7] J. C. Comiso, P. Wadhams, L. T. Pedersen, and R. A. Gersten. Seasonal and interannual variability of the odden ice tongue and a study of environmental effects. *Journal of Geophysical Research*, 106(C5):9093–9116, May 2001.
- [8] P. Gloersen, W. J. Campbell, D. J. Cavalieri, J. C. Comiso, C. L. Parkinson, and H. J. Zwally. *Arctic and Antarctic Sea Ice 1978-1987: Satellite passive-microwave observations and analysis*. National Aeronautics and Space Administration, Washington, D.C., 1992.
- [9] Norwegian Meteorological Institute. klima: External access to climatedata from norwegian meteorological institute. Available from <http://eklima.met.no>.
- [10] P. D. Killworth. On “chimney” formation in the ocean. *Journal of Physical Oceanography*, 9(3):531–554, May 1979.
- [11] M. Leppäranta and W. D. Hibler III. Mesoscale sea ice deformation in the east greenland marginal ice zone. *Journal of Geophysical Research*, 92(C7):7060–7070, June 1987.
- [12] T. Markus and D. Cavalieri. An enhancement of the NASA Team sea ice algorithm. *IEEE Transactions on Geoscience and Remote Sensing*, 38:1387–1398, 2000.
- [13] J. Marshall and F. Schott. Open-ocean convection observations, theory and models. *Reviews of Geophysics*, 37(1):1–64, February 1999.
- [14] C. L. Parkinson, J. C. Comiso, H. J. Zwally, D. J. Cavalieri, P. Gloersen, and W. J. Campbell. *Arctic Sea Ice, 1973-1976: Satellite passive-microwave observations*. National Aeronautics and Space Administration, Washington, D.C., 1987.
- [15] J. Rodrigues. The rapid decline of the sea ice in the russian arctic. *Cold Regions Science and Technology*, 2008.
- [16] Y. Seleshi, G. R. Demaree, and J. W. Delleur. Sunspot numbers as a possible indicator of annual rainfall at Addis Ababa, Etheopia. *International Journal of Climatology*, 14:911–923, 1994.
- [17] R. A. Shuchman, E. G. Josberger, C. A. Russel, K. W. Fischer, O. M. Johannessen, J. Johannessen, and P. Gloersen. Greenland Sea Odden sea ice feature: Intra-annual and interannual variability. *Journal of Geophysical Research*, 103(6):12709–12724, 1998.
- [18] J. Stroeve, M. M. Holland, W. Meier, T. Scambos, and M. Serreze. Arctic sea ice decline: Faster than forecast. *Geophysical Research Letters*, 34:L09501, May 2007.
- [19] D. W. J. Thompson and J. M. Wallace. Annular modes in the extratropical circulation. Part I: Month-to-month variability. *Journal of Climate*, 13(5):1000–1016, March 2000.
- [20] D. W. J. Thompson and J. M. Wallace. Indices of the annular modes, 2000. Available at www.ao.atmos.colostate.edu/Data/ao_index.html.
- [21] L. Toudal. Ice extent in the Greenland Sea 1978-1995. *Deep-Sea Reserach II*, 46:1237–1254, 1999.
- [22] H. Tuomenvirta, A. Drebs, E. Forland, O. E. Tveito, H. Alexandersson, E. V. Laursen, and T. Jonsson. Nordklim data set 1.0, 2001. Available from www.smhi.se/hfa_coord/nordklim.
- [23] CSIRO (Scientific UK Meteorological Office, Hadley Centre, Australia Industrial Research for Australia), NIWA (National Institute of Water, and New Zealand Atmospheric Research). Met office - global mean sea-level pressure datasets (GMSLP and HadSLP1). Internet, 2000. Available from <http://badc.nerc.ac.uk/data/gmslp/>.
- [24] UEA Climate Research Unit. Nao dataset, 2000. Available at www.cru.uea.ac.uk/cru/data/nao.htm.
- [25] M. Visbeck, J. Fischer, and F. Schott. Preconditioning the Greenland Sea for deep convection: Ice formation and ice drift. *Journal of Geophysical Research*, 100(C9):18,489–18,502, September 1995.
- [26] P. Wadhams, J. C. Comiso, E. Prussen, S. Wells, M. Brandon, E. Aldworth, T. Viehoff, R. Allegrino, and D. R. Crane. The development of the Odden ice tongue in the Greenland Sea during winter 1993 from remote sensing and field observations. *Journal of Geophysical Research*, 101(C8):18,213–18,235, August 1996.
- [27] P. Wadhams and J. P. Wilkinson. The physical properities of sea ice in the Odden ice tongue. *Deep-Sea Research II*, 46:1275–1300, 1999.
- [28] J. P. Wilkinson and P. Wadhams. A method of detecting changes in ice conditions of the central Greenland Sea by whelping locations of harp seals. *Journal of Climate*, 18(8):1216–1226, April 2005.